

β -functions in large- N_f supersymmetric gauge theories

P.M. Ferreira, I. Jack, D.R.T. Jones and C.G. North

Dept of Mathematical Sciences, University of Liverpool, Liverpool L69 3BX, U.K.

We present calculations of the leading and $O(1/N_f)$ terms in a large- N_f expansion of the β -functions and anomalous dimensions for various supersymmetric gauge theories, including supersymmetric QCD. In the case of supersymmetric QCD, we show that our $O(1/N_f)$ approximation displays an infra-red fixed point in the conformal window $\frac{3}{2}N_c < N_f < 3N_c$.

1. Introduction

The large- N expansion is an alternative to conventional perturbation theory. In both QCD and supersymmetric QCD (SQCD), the large N_c expansion is of particular interest [1]; more tractable, however is the large N_f expansion, and it is this that we study here, for SQCD. In any theory, calculation correct to some non-trivial order in $1/N$ requires the summation of one or more infinite sets of Feynman diagrams, and hence possible insight into the large-order behaviour of perturbation theory. There is a considerable literature devoted to the study of large order perturbation theory [2], but remarkably little of it concerned with supersymmetric theories. [For a discussion of the large order behaviour of the supersymmetric anharmonic oscillator, see Ref. [3]; and for investigation of the role of renormalons in various supersymmetric theories see Ref. [4]. Supersymmetric σ -models have been studied at large N using critical methods [5] in a series of papers by Gracey: see for example Ref. [6].] In this paper we calculate the leading and $O(1/N_f)$ terms in the gauge beta-function, β_g , for SQCD¹. The type of bubble-sums we confront are in fact similar to those in Ref. [4]; the difference being that they were concerned with renormalon singularities in amplitudes, whereas, our interest being in beta-functions, we require the ultra-violet divergent terms from such sums. We find that all our results can be expressed in terms of a simple function of the coupling constant, and that although infinite classes of diagrams have been summed, the resulting coefficient of $1/N_f$ has a finite radius of convergence in g . Of course we cannot expect the expansion in powers of $1/N_f$ to be convergent; it might well, however, be Borel-summable, as has been conjectured[8] for the expansion in g .

Some of our results have already appeared in Ref. [9]; here we give more calculational detail and also extract the SQCD case. We use the superfield formalism, allied with supersymmetric dimensional regularisation and minimal subtraction (DRED)[10]. As always with superfield perturbation theory, the calculation of a typical contribution consists of first reducing a superfield Feynman diagram to a normal one by performing D -algebra, and then performing the resulting Feynman integral. The first part is straightforward, because our diagrams consist of bubble chains grafted on to otherwise (at most) three-loop graphs. The second part appears formidable; but fortunately the key to its performance has been provided by Palanques-Mestre and Pascual[11], who carried out similar non-supersymmetric calculations in the abelian case. The crucial realisation is that the automatic cancellation

¹ For QCD at large N_f see [7]

of non-local counter-terms leads to apparently miraculous (but easily verified) identities which simplify the summation over subtractions.

In the next section we carry out our program for an Abelian theory, with a superpotential selected so that $\mathcal{N} = 2$ supersymmetry is included as a special case. Then in section 3 we show how with very little extra work we can extract the corresponding result for the non-Abelian case, by exploiting the fact that $\mathcal{N} = 2$ theories are finite beyond one loop. In section 4 we show how the SQCD result can be also deduced, and in section 5 we compare our result with perturbation theory in g for the SQCD case.

2. General Abelian Theory

Here we present results for a general theory produced by a U_1 gauging of the Wess-Zumino model with a superpotential given by

$$W = \frac{\lambda}{\sqrt{N_f}} \sum_{i=1}^{N_f} \phi \xi_i \chi_i. \quad (2.1)$$

Suppose we require a gauging such that the charges $q_{\chi_i} \equiv q_\chi$ and $q_{\xi_i} \equiv q_\xi$ are independent of i . Charge conservation and anomaly cancellation then require

$$q_\phi + q_\chi + q_\xi = q_\phi^3 + N_f(q_\chi^3 + q_\xi^3) = 0, \quad (2.2)$$

yielding

$$(N_f - 1)(q_\chi^3 + q_\xi^3) - 3(q_\chi^2 q_\xi + q_\chi q_\xi^2) = 0. \quad (2.3)$$

An obvious solution is $q_\xi = -q_\chi$, $q_\phi = 0$. In fact if this does not hold, then dividing Eq. (2.3) by $q_\chi + q_\xi$ we obtain

$$(N_f - 1)(q_\chi^2 + q_\xi^2) - (N_f - 2)q_\chi q_\xi = 0, \quad (2.4)$$

which is easily seen to have no solutions (except in the case $N_f = 1$, with either $q_\xi = 0$ or $q_\chi = 0$, which are clearly not interesting from our present large- N_f perspective). So we now set $q_\phi = 0$ and $q_\xi = -q_\chi = q$; we will take $q = g/\sqrt{N_f}$. For the special case $\lambda = \sqrt{2}g$ we have $\mathcal{N} = 2$ supersymmetry. In Fig. 1 we show the Feynman diagrams we require for β_g .

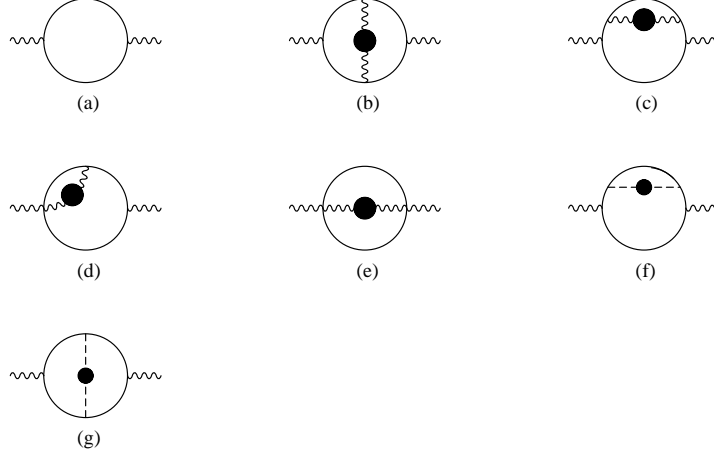


Fig. 1: Feynman diagrams for section 2. Wavy lines are vector propagators, solid lines are ξ or χ propagators, and dashed lines are ϕ propagators. Blobs denote sums of chains of ξ, χ bubbles.

A blob on a diagram represents the sum of chains of ξ, χ bubbles of arbitrary length, as shown in Fig. 2(a) (for a ϕ -propagator) and Fig. 2(b) (for a vector propagator). We choose to work in the Landau gauge; this means that the diagram with no bubble on a vector propagator can be subsumed with the diagrams with chains of bubbles, since a chain of one or more bubbles produces a transverse projection operator. Fig. 1(a) is $O(1)$, while Figs. 1(b)-(g) are all $O(1/N_f)$.

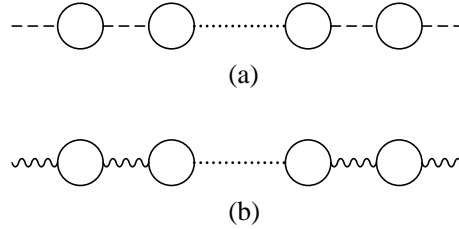


Fig. 2: Bubble chains on chiral and vector propagators.

For details of our technique for dealing with the D -algebra part of the calculation we refer the reader to Ref. [12], where we found β_g for an abelian theory to four loops by calculating the vector superfield self-energy. The upshot is that each diagram with a blob reduces to one of a basic set of Feynman integrals, depicted in Fig. 3. Again in Fig. 3, a chain of bubbles is understood to represent a summation over arbitrary numbers of bubbles.

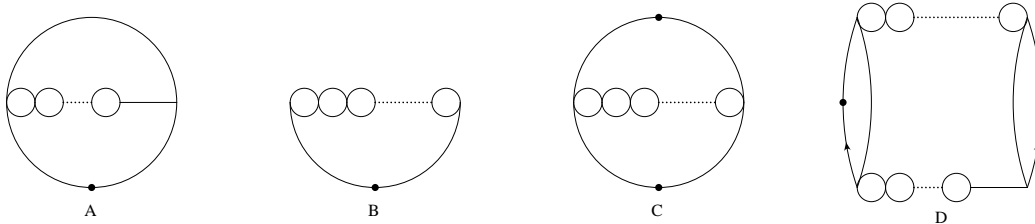


Fig. 3: Feynman diagrams representing the bubble sums A, B C and D. The black dots denote squared propagators and pairs of arrows denote contracted momenta.

The Feynman integrals (A)-(D) are evaluated in Appendix A, with results given in Eqs. (A.17), (A.8), (A.18) and (A.25) respectively. We note all the bubble sums relevant to our calculations depend on the function $G(x)$, which has a zero at $x = 1$ and a simple pole at $x = \frac{3}{2}$. We may therefore anticipate that our results in this and subsequent sections will have a finite radius of convergence in the appropriate coupling constant, because of this pole. The contributions from the diagrams in Fig. 1 are given in terms of the diagrams of Fig. 3 in Table 1. In this Table and the following ones, the second column represents the result of performing the D -algebra, and should be multiplied by the corresponding factor in the third column which represents the symmetry factor and also (in the non-abelian case) products of group matrices. An additional factor of $1/N_f$ is also understood in each case, and we have introduced $K = g^2/(8\pi^2)$ and $y = \lambda^2/(16\pi^2)$. For $\mathcal{N} = 2$ supersymmetry we have $y = K$.

Diagram	Bubble Sum	Factor
1(b)	$\frac{1}{2}C(K) - 2A(K)$	$2gK^2$
1(c)	$\frac{1}{2}[\frac{1}{K}B(K) - A(K)]$	$4gK^2$
1(d)	$\frac{1}{2}[\frac{1}{K}B(K) - A(K)]$	$-8gK^2$
1(e)	$\frac{1}{K}B(K)$	$2gK^2$
1(f)	$A(y)$	$2gKy$
1(g)	$C(y)$	$-gKy$

Table 1: $O(1/N_f)$ contributions to β_g for the abelian theory.

Figs. 1(b)-1(g) evidently have precise counterparts in a three-loop calculation with the blob representing just one bubble; and in fact the bubble-summed diagrams (A)-(D) of

Fig. 3 are generalised forms of those in Fig 2(A)-(D) of Ref. [12]. The results in Table 1 for Figs. 1(b)-1(g) can hence be read off from the corresponding results of Table 1 in Ref. [12]. Using our results from Appendix A for Fig. 3(A)-(D) and including the $O(1)$ contribution of Fig. 1(a), we obtain

$$\beta_g = gK \left[1 + \frac{2}{N_f} \int_y^K (1-2x)G(x) dx \right]. \quad (2.5)$$

The anomalous dimensions through $O(1/N_f)$ are given by Fig. 4.

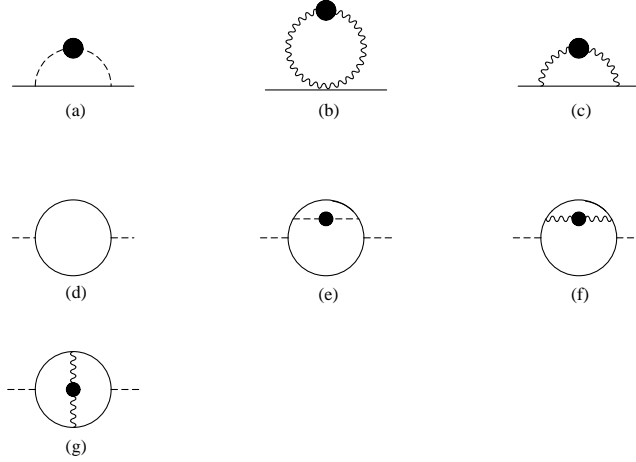


Fig. 4: Feynman diagrams for the anomalous dimensions

The contributions from these diagrams are given in Table 2, in terms of the basic diagrams of Fig. 3.

Diagram	Bubble Sum	Factor
4(a)	$B(y)$	y
4(b)	$B(K)$	$-K$
4(c)	0	
4(e)	$A(y)$	$2y^2$
4(f)	$\frac{1}{K}[B(K) - 1] - A(K)$	$2yK$
4(g)	$\frac{1}{K}[B(K) - 1]$	$-2yK$

Table 2: $O(1/N_f)$ contributions to anomalous dimensions for the abelian theory

The contributions from graphs with one or more bubbles in Fig. 4(c) are guaranteed to be zero since the bubbles lead to a transverse projection operator on the vector propagator,

giving zero when attached to an external line. Since we have chosen the Landau gauge, the zero-bubble contribution to Fig. 4(c) will also give zero by the same token. The same reasoning will be used later to deduce that Figs. 6(b),(d) give zero. Adding the contributions from Figs. 4(a)-(c), and those from Figs. 4(d)-(g), we obtain

$$\begin{aligned}\gamma_\xi = \gamma_\chi &= \frac{1}{N_f} [yG(y) - KG(K)], \\ \gamma_\phi &= y + \frac{2y}{N_f} \left[G(K) - G(y) + 2 \int_y^K G(x) dx \right].\end{aligned}\tag{2.6}$$

It is easy to verify that our result for β_g in Eq. (2.5) reproduces the relevant terms in the three and four loop calculations presented in Ref. [12]. The results for $\gamma_{\xi,\chi}$ and γ_ϕ in Eq. (2.6) agree with the three-loop results of Ref. [13], and in the ungauged case agree with the four-loop results of Ref. [14] for a generalised Wess-Zumino model. Moreover, for $\mathcal{N} = 2$ (which corresponds to $y = K$) we have $\beta_g = \gamma_\phi = 0$ beyond one loop, and $\gamma_\xi = \gamma_\chi = 0$ to all orders, in accordance with Ref. [15]. The results of Eqs. (2.5), (2.6) may readily be specialised to the case of supersymmetric QED simply by setting $y = 0$.

3. General Non-Abelian Theory

We now consider a non-abelian theory with gauge group \mathcal{G} and superpotential

$$W = \frac{\lambda}{\sqrt{N_f}} \phi^a \sum_{i=1}^{N_f} \xi_i^T S_a \chi_i,\tag{3.1}$$

where ξ_i, χ_i, ϕ are multiplets transforming under the S^*, S and adjoint representations of \mathcal{G} respectively. For notational simplicity we take the representation S to be irreducible for the time being; we shall present the results for a reducible representation in due course. In addition to diagrams similar in form to those computed earlier in the abelian case and shown in Fig. 1, the two-point function for the vector superfield includes the additional diagrams depicted in Fig. 5, because the ϕ field now has gauge interactions. There are also further diagrams involving the gauge coupling g only, which we shall be able to avoid computing.

The diagrams of Figs. 1(f),(g) and Fig. 5 contain no internal vectors, and produce contributions to β_g which contain the Yukawa coupling y (apart from the zero-bubble contribution to Fig. 5(a)). They are in fact the only graphs which contribute y dependent

terms up to $O(1/N_f)$. Graphs with no vector propagators will be the same in the background field gauge as in an ordinary gauge. Now in the background field gauge, β_g is given by the vector-field two-point function even in the non-abelian case. We deduce that the contribution to β_g at $O(1/N_f)$ which contains y is correctly given by Figs. 1(f),(g) and Fig. 5. Upon performing the D -algebra, these diagrams all give rise to Feynman integrals with bubble sums as depicted in Fig. 3. The contributions from the diagrams of the form Figs. 1(f),(g) and Fig. 5 are listed in Table 3.

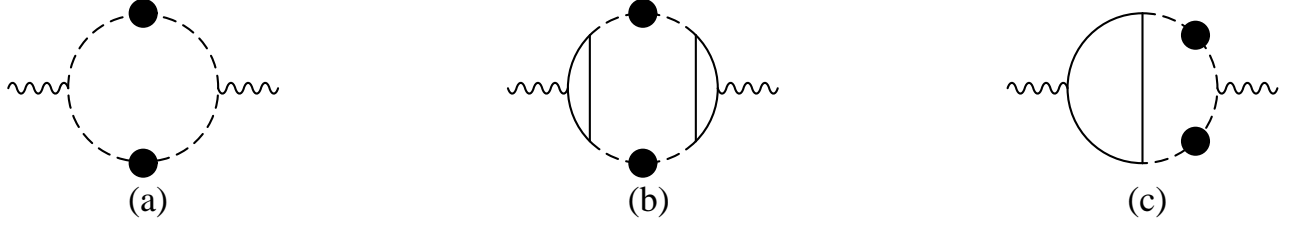


Fig. 5: Additional vector two-point diagrams for the non-abelian theory.

Diagram	Bubble Sum	Group factor
1(f)	$A(\hat{y})$	$2gK\hat{y}C_S$
1(g)	$C(\hat{y})$	$-gK\hat{y}[C_S - \frac{1}{2}C(G)]$
5(a)	$\hat{B}(\hat{y})$	$\frac{1}{2}gKC(G)$
5(b)	$-\tilde{B}(\hat{y}) - 2D(\hat{y})$	$\frac{1}{2}gK\hat{y}^2C(G)$
5(c)	0	

Table 3: $O(1/N_f)$ contributions to β_g in the non-abelian theory.

The second column of Table 3 requires some explanation. Firstly, we have defined $\hat{y} = yT(S)$, where $T(S)\delta_{ab} = \text{tr}(S_a S_b)$. Secondly, care needs to be taken with the graphs of Fig. 5, which contain two bubble-chains. This leads to extra combinatorial factors. In fact, upon performing the D -algebra, Fig. 5(a) yields a Feynman integral with the topology of Fig. 3(B), but the calculation differs from that in Appendix A, in that Eq. (A.8) is replaced by

$$B(\kappa) \rightarrow \hat{B}(\kappa) = \sum_{n=0}^{\infty} (n+1)G_n \kappa^n = \frac{d}{d\kappa} [\kappa G(\kappa)]. \quad (3.2)$$

Similarly, Fig. 5(b) yields two Feynman integrals. One again has the topology of Fig. 3(B), but now with

$$B(\kappa) \rightarrow \tilde{B}(\kappa) = \sum_{n=0}^{\infty} (n+1)G_{n+2} \kappa^n = \frac{d}{d\kappa} \left\{ \frac{1}{\kappa} [G(\kappa) - 1] \right\}. \quad (3.3)$$

The other is depicted in Fig. 3(D), and yields a bubble-sum contribution given in Eq. (A.25). In the third column, we have defined $C(S) = C_S 1$, where $C(S) = S_a S_a$, and used $\frac{\text{tr}[C(S)^2]}{rT(S)} = C_S$ for an irreducible representation (where r is the number of group generators). Adding the contributions in Table 3, we find

$$-\frac{2gKC_S}{N_f} \int_0^{\hat{y}} (1-2x)G(x) dx + \frac{gK}{N_f} \left[\frac{1}{2} - \int_0^{\hat{y}} G(x) dx \right] C(G). \quad (3.4)$$

As argued earlier, this represents the full y -dependent contribution at $O(1/N_f)$, together with a single y -independent term which represents the (one-loop) contribution from the zero-bubble part of Fig. 5(a). We can then infer the full non-abelian result by using the afore-mentioned fact that there are no divergences beyond one loop for $\mathcal{N} = 2$, i.e. when we set $y = K$, together with the fact that the part of β_g we have not yet calculated is purely a function of g . We also need to include the rest of the one-loop β_g . The result is

$$\begin{aligned} \beta_g = & gK \left[T(S) + \frac{2C_S}{N_f} \int_{\hat{y}}^{\hat{K}} (1-2x)G(x) dx \right] \\ & + \frac{gK}{N_f} \left[\int_{\hat{y}}^{\hat{K}} G(x) dx - 1 \right] C(G), \end{aligned} \quad (3.5)$$

where $\hat{K} = KT(S)$.

The chiral superfield anomalous dimensions are given by diagrams of the form of Fig. 4 together with the additional diagrams of Fig. 6.

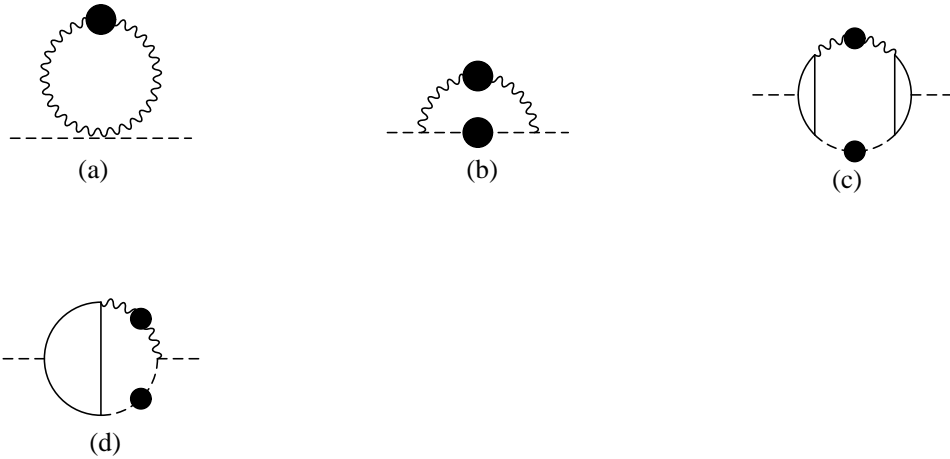


Fig. 6: The additional Feynman diagrams for the anomalous dimension in the non-abelian theory.

The individual contributions at $O(1/N_f)$ are given in Table 4.

Diagram	Bubble Sum	Group factor
4(a)	$B(\hat{y})$	$yC(S)$
4(b)	$B(\hat{K})$	$-KC(S)$
4(c)	0	
4(e)	$A(\hat{y})$	$2y\hat{y}C_S$
4(f)	$\frac{1}{\hat{K}}[B(\hat{K}) - 1] - A(\hat{K})$	$2y\hat{K}C_S$
4(g)	$\frac{1}{\hat{K}}[B(\hat{K}) - 1]$	$-2y\hat{K}[C_S - \frac{1}{2}C(G)]$
6(a)	$B(\hat{K})$	$-KC(G)$
6(b)	0	
6(c)	0	
6(d)	0	

Table 4: $O(1/N_f)$ contributions to anomalous dimensions for the non-abelian theory.

The anomalous dimensions for ξ or χ are given at $O(1/N_f)$ by adding the contributions from Figs. 4(a)-(c), while the anomalous dimension for ϕ is given up to $O(1/N_f)$ by adding the $O(1/N_f)$ contributions from Figs. 4(e)-(g), and Figs. 6(a)-(c), together with the $O(1)$ contribution from Fig. 4(d). We obtain:

$$\gamma_\xi = \gamma_\chi = \frac{1}{N_f} \left[yG(\hat{y}) - KG(\hat{K}) \right] C(S), \quad (3.6a)$$

$$\begin{aligned} \gamma_\phi = \hat{y} + \frac{2yC_S}{N_f} \left[G(\hat{K}) - G(\hat{y}) + 2 \int_{\hat{y}}^{\hat{K}} G(x) dx \right] \\ + \frac{1}{N_f} (y - K)G(\hat{K})C(G) - \frac{y}{N_f}C(G). \end{aligned} \quad (3.6b)$$

The above results contain as special cases all those presented in previous sections. Once again one can check compatibility with the three and four-loop calculations from Ref. [12] and Ref. [13].

For completeness we present results for the case when χ, ξ transform according to a *reducible* representation. Suppose there are n_α pairs of multiplets $\xi_{i_\alpha}^\alpha, \chi_{i_\alpha}^\alpha$, each transforming according to a representation S^α , and with $\sum_\alpha n_\alpha = N_f$. The superpotential becomes:

$$W = \sum_\alpha \sum_{i_\alpha=1}^{n_\alpha} \frac{\lambda_\alpha}{\sqrt{N_f}} \phi^a \xi_{i_\alpha}^\alpha{}^T S_a^\alpha \chi_{i_\alpha}^\alpha, \quad (3.7)$$

where α labels the irreducible representations. It is convenient to generalise the definitions of \hat{y} and \hat{K} as follows:

$$\begin{aligned}\hat{y} &= \frac{1}{N_f} \sum_{\alpha} n_{\alpha} y_{\alpha} T(S_{\alpha}) \\ \hat{K} &= \frac{g^2}{8\pi^2 N_f} \sum_{\alpha} n_{\alpha} T(S_{\alpha})\end{aligned}\tag{3.8}$$

and introduce

$$\begin{aligned}\Delta_K &= \frac{K}{r N_f} \sum_{\alpha} n_{\alpha} \text{Tr} [C(S_{\alpha})^2] \\ \Delta_y &= \frac{1}{r N_f} \sum_{\alpha} n_{\alpha} y_{\alpha} \text{Tr} [C(S_{\alpha})^2] \\ \Delta_{y^2} &= \frac{1}{r N_f} \sum_{\alpha} n_{\alpha} y_{\alpha}^2 \text{Tr} [C(S_{\alpha})^2].\end{aligned}\tag{3.9}$$

Our results are:

$$\begin{aligned}\frac{\beta_g}{g} &= \hat{K} + \frac{2K\Delta_K}{N_f \hat{K}} \int_0^{\hat{K}} (1-2x)G(x) dx - \frac{2K\Delta_y}{N_f \hat{y}} \int_0^{\hat{y}} (1-2x)G(x) dx \\ &\quad + \frac{K}{N_f} C(G) \left[\int_{\hat{y}}^{\hat{K}} G(x) dx - 1 \right], \\ \gamma_{\xi_{\alpha}} &= \gamma_{\chi_{\alpha}} = \frac{1}{N_f} \left[y_{\alpha} G(\hat{y}) - K G(\hat{K}) \right] C(S_{\alpha}), \\ \gamma_{\phi} &= \hat{y} + \frac{2\Delta_y K}{N_f \hat{K}} \left[G(\hat{K}) - 1 + 2 \int_0^{\hat{K}} G(x) dx \right] \\ &\quad - \frac{2\Delta_{y^2}}{N_f \hat{y}} \left[G(\hat{y}) - 1 + 2 \int_0^{\hat{y}} G(x) dx \right] \\ &\quad + \frac{K \hat{y}}{N_f \hat{K}} C(G) \left[G(\hat{K}) - 1 \right] - \frac{K}{N_f} G(\hat{K}) C(G).\end{aligned}\tag{3.10}$$

4. Supersymmetric QCD

We can now deduce β_g and the chiral superfield anomalous dimension for large- N_f supersymmetric QCD from the results of the previous section. We consider supersymmetric QCD with N_f pairs of chiral superfields ξ_i, χ_i , transforming under the S^*, S representations of \mathcal{G} respectively. In principle, to obtain the results for supersymmetric QCD from those for our general non-abelian theory, we need to remove the contributions of all diagrams

involving the adjoint field ϕ . For the anomalous dimension of the chiral field, we simply need to remove the diagram Fig. 4(a). The result is then

$$\gamma_\xi = \gamma_\chi = -\frac{1}{N_f} K G(\hat{K}) C(S). \quad (4.1)$$

We note that we may obtain this result simply by setting $y = 0$ in Eq. (3.6a). In fact, the same principle may also be applied in the case of β_g . One can convince oneself that the vector-field two-point diagrams with a ϕ -propagator which contribute at $O(1/N_f)$ are precisely those of Fig. 1(f),(g) and Fig. 5. These all contain y except for the zero-bubble contribution to Fig. 5(a). Hence, we can delete the contributions of diagrams with adjoint fields simply by setting $y = 0$ in Eq. (3.5), provided we also subtract the contribution of the zero-bubble contribution to Fig. 5(a) (i.e. the y -independent term in Eq. (3.4)) by hand. The result is

$$\begin{aligned} \beta_g = & gK \left[T(S) + \frac{2C_S}{N_f} \int_0^{\hat{K}} (1-2x) G(x) dx \right] \\ & + \frac{gK}{N_f} \left[\int_0^{\hat{K}} G(x) dx - \frac{3}{2} \right] C(G). \end{aligned} \quad (4.2)$$

For the case of $SU(N_c)$ with N_f flavours we find

$$\begin{aligned} \beta_g = & \frac{1}{2} gK - \frac{3N_c}{2N_f} gK + 2gK \frac{N_c}{N_f} \int_0^{\hat{K}} (1-x) G(x) dx \\ & - \frac{gK}{N_c N_f} \int_0^{\hat{K}} (1-2x) G(x) dx. \end{aligned} \quad (4.3)$$

Note that in this case $\hat{K} = K/2$.

It is also of interest to consider the case of supersymmetric QCD coupled to a singlet ϕ by a superpotential

$$W = \frac{\lambda}{\sqrt{N_f}} \phi \sum \xi_i^T \chi_i. \quad (4.4)$$

The additional diagrams contributing to the vector two-point function are of the form of Figs. 1(f),(g). Now these diagrams contain no internal vectors, and hence would be the same in the background field gauge as in a conventional gauge. But in the background gauge, β_g is determined by the vector two-point diagrams. Hence the additional contribution to β_g can be computed from these diagrams. The contributions can be read off from

the corresponding entries in Table 1 by replacing K by \hat{K} in the last column. Hence β_g is now given by

$$\begin{aligned}\beta_g = & g\hat{K} \left[1 - \frac{2}{N_f} \int_0^y (1-2x)G(x) dx \right] + \frac{2gKC_S}{N_f} \int_0^{\hat{K}} (1-2x)G(x) dx \\ & + \frac{gK}{N_f} \left[\int_0^{\hat{K}} G(x) dx - \frac{3}{2} \right] C(G).\end{aligned}\tag{4.5}$$

The anomalous dimensions are now given by diagrams of the form Fig. 4. The contributions from Figs. 4(a)-(c) can be read off from the corresponding entries in Table 2 by replacing K by \hat{K} in the second column and by $KC(S)$ in the third column, giving

$$\gamma_\xi = \gamma_\chi = \frac{1}{N_f} \left[yG(y) - KG(\hat{K})C(S) \right]\tag{4.6}$$

The contributions from Figs. 4(e)-(g) can be read off from Table 2 by replacing K by \hat{K} everywhere, giving

$$\gamma_\phi = y + \frac{2y}{N_f} \left[G(\hat{K}) - G(y) + 2 \int_y^{\hat{K}} G(x) dx \right].\tag{4.7}$$

For the case of $SU(N_c)$ with N_f flavours we find

$$\begin{aligned}\beta_g = & \frac{1}{2}gK - \frac{3N_c}{2N_f}gK + 2gK\frac{N_c}{N_f} \int_0^{\hat{K}} (1-x)G(x) dx \\ & - \frac{gK}{N_cN_f} \int_0^{\hat{K}} (1-2x)G(x) dx - \frac{gK}{N_f} \int_0^y (1-2x)G(x) dx.\end{aligned}\tag{4.8}$$

5. Infra-red fixed points

In this section we compare our result for supersymmetric QCD with perturbation theory in the gauge coupling. We begin by giving the known results at one through three loops: ²

$$\begin{aligned}16\pi^2\beta_g^{(1)} &= \left(1 - 3\frac{N_c}{N_f} \right) g^3, \\ (16\pi^2)^2\beta_g^{(2)} &= \left(\left[4N_c - \frac{2}{N_c} \right] \frac{1}{N_f} - 6\frac{N_c^2}{N_f^2} \right) g^5, \\ (16\pi^2)^3\beta_g^{(3)} &= \left(\left[\frac{3}{N_c} - 4N_c \right] \frac{1}{N_f} + \left[21N_c^2 - \frac{2}{N_c^2} - 9 \right] \frac{1}{N_f^2} - 21\frac{N_c^3}{N_f^3} \right) g^7.\end{aligned}\tag{5.1}$$

² Recall that our gauge coupling is $g/\sqrt{N_f}$

For $\beta_g^{(4)}$ we have only a partial result[13]:

$$(16\pi^2)^4 \beta_g^{(4)} = \left(-\frac{2}{3} \frac{1}{N_c N_f} + \left[-\left(\frac{62}{3} + 2\kappa + 8\alpha \right) N_c^2 + \frac{100}{3} + 4\alpha + \frac{6\kappa - 20}{3N_c^2} \right] \frac{1}{N_f^2} \right. \\ \left. + \left[36(1 + \alpha) N_c^3 - (34 + 12\alpha) N_c - \frac{8}{N_c} - \frac{4}{N_c^3} \right] \frac{1}{N_f^3} - (6 + 36\alpha) \frac{N_c^4}{N_f^4} \right) g^9 \quad (5.2)$$

where α is an as yet undetermined parameter, and where $\kappa = 6\zeta(3)$.

It is easy to show[16] that $\beta_g^{(2)} > 0$ when $\beta_g^{(1)} = 0$. For $\beta_g^{(1)}$ less than but near zero, it follows that there exists an infra-red fixed point in the evolution of g under renormalisation³. According to Seiberg[18] this fixed point in fact exists for the conformal window $\frac{3}{2}N_c < N_f < 3N_c$. Our expansion clearly demands $N_f \gg N_c$ and so places the theory firmly in the weakly coupled infra-red free regime; nevertheless it is tempting to compare our result Eq. (4.3) with perturbation theory for a value of N_f in the conformal window.

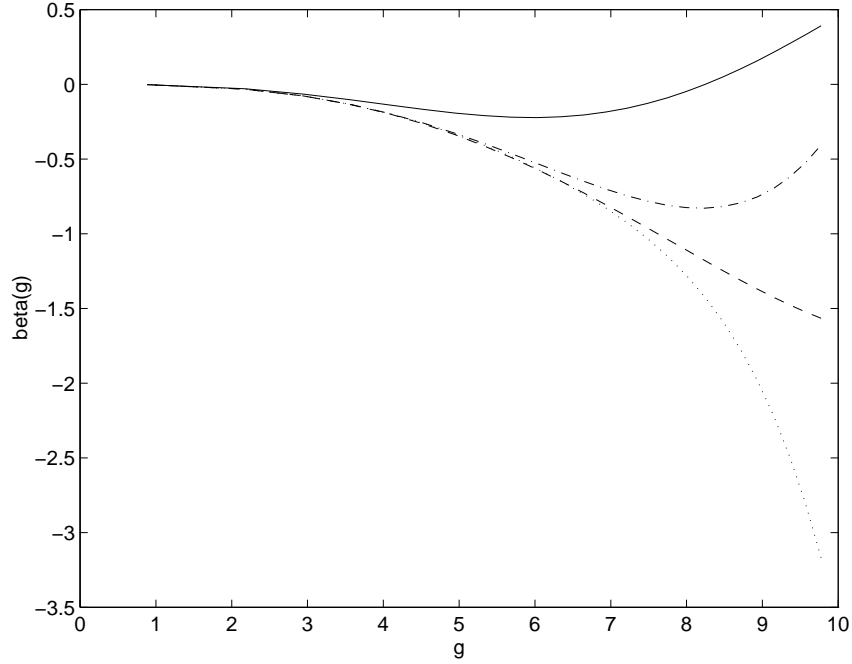


Fig. 7: Comparison between Eq. (4.3) (solid line) and the two, three and four loop approximations for β_g (dashed, dot-dashed and dotted lines respectively), for $N_c = 3$ and $N_f = 6$.

In Fig. 7 we plot β_g against g using 2...4-loop perturbation theory and our result Eq. (4.3) for $N_c = 3$ and $N_f = 6$. In the case of $\beta_g^{(4)}$ we have set $\alpha = 0$; based on Ref. [13]

³ This holds also for non-supersymmetric QCD [17]

we would anticipate that $|\alpha|$ is $O(1)$, and the evolution is insensitive to the value of α in this region. The IR fixed point occurs at $g \approx 8$; of course this result is scheme dependent, but it is interesting that it is substantially smaller than that obtained in either the two or the three loop approximation; the four loop approximation does not give a fixed point at all (unless α is large and positive).

6. Discussion

It is quite remarkable that the $O(1/N_f)$ corrections to the SQCD β_g depend only on simple integrals involving $G(x)$. G has a simple pole at $x = 3/2$ and consequently β_g has a logarithmic singularity at $g^2/(16\pi^2) = 3/2$ and a finite radius of convergence in g . We have found that for values of N_f, N_c corresponding to the conformal window $3N_c/2 < N_f < 3N_c$, there indeed exists an infra-red fixed point in the gauge coupling evolution, though as we emphasised this regime is clearly outside the region of strict validity of our approximation.

If we had some more terms in the $1/N_f$ expansion, we could try Padé or Borel-Padé techniques and continue to small N_f . This might permit us to extend the radius of convergence mentioned above, and also investigate more reliably the conformal window $3N_c/2 < N_f < 3N_c$. Even the $O(1/N_f^2)$ contribution presents considerable technical problems, however. It is interesting to note that this calculation would suffice to determine the unknown parameter α in Eq. (5.2), and consequently complete the derivation of $\beta_g^{(4)}$ carried out in Ref. [13]. Perhaps the critical methods of Ref [5] could be extended to superfields and facilitate such calculations. It may also be possible to determine α [19] using Padé approximants[20]. It would be interesting to see whether the finite radius of convergence in g which we noted above persists at higher orders in $1/N_f$. In fact, it is natural to speculate that the $O(1/N_f^2)$ term, for instance, would depend on G^2 , or some convolution thereof.

Since our calculations involve contributions from all orders in perturbation theory, we should address the question of ambiguities in DRED[21] which can potentially arise at higher orders. In our earlier paper on the present topic[9], we argued that the particular graphs we consider, consisting of bubble chains inserted onto simple lower order graphs, are unambiguous; we also speculated that any DRED ambiguities present in the theory as a whole should be equivalent to renormalisation scheme ambiguities and as such can be subsumed into coupling constant redefinitions.

Appendix A. Bubble sums

In this appendix we give details of our bubble-sum calculations for the diagrams of Fig. 3. We do all calculations with zero external momentum, using supersymmetric dimensional regularisation (with $d = 4 - 2\epsilon$) and minimal subtraction (DRED)[10]. By performing subtractions at the level of the Feynman integrals we completely separate the calculation of the (subtracted) Feynman integrals from the details of the theory under consideration. It is convenient to redefine the d -dimensional integration measure so that

$$\int \frac{d^d k}{k^2(k-p)^2} = \pi^2 \frac{1}{\epsilon} (p^2)^{-\epsilon}. \quad (\text{A.1})$$

The diagrams we will require are shown in Figure 3. Let us consider Fig. 3(B) first of all, as this is the simplest integral to evaluate. As explained in the main text, this diagram represents a sum over chains of bubbles of arbitrary length. The n -bubble diagram, before subtracting subdivergences, produces a contribution

$$\frac{\kappa^n}{\epsilon^{n+1}} G(\epsilon) \frac{1 - (n+1)\epsilon}{n+1} \Gamma[1 + (n+1)\epsilon] \Gamma[1 - (n+1)\epsilon] x^{(n+1)\epsilon} \quad (\text{A.2})$$

where

$$G(\epsilon) = \frac{\Gamma(2 - 2\epsilon)}{\Gamma(2 - \epsilon)\Gamma(1 - \epsilon)^2\Gamma(1 + \epsilon)} \quad (\text{A.3})$$

and $x = \mu^{-2}$, μ being the regulator mass. The parameter κ subsumes any constant factors which will recur on a bubble-by-bubble basis, including a factor of $(16\pi^2)^{-1}$ for each bubble. Since this is an $(n+1)$ -loop diagram, there remains an additional factor of $(16\pi^2)^{-1}$ which we have included in the third columns of the Tables in the main text. Similar considerations will apply to Figs. (A),(C), and (D). We must now subtract diagrams with counterterm insertions corresponding to each divergent subdiagram. For the n -bubble contribution, the divergent subdiagrams consist of subsets of $n - r + 1$ bubbles, where $1 \leq r \leq n$ (not necessarily forming a continuous chain). Such a subdiagram yields a counterterm of $\frac{(-1)^{n-r}\kappa^{n-r+1}}{\epsilon^{n-r+1}}$, after subtracting all its own subdivergences. The remaining $(r-1)$ -bubble diagram gives a contribution as in Eq. (A.2), but with n replaced by $r-1$. Taking into account a combinatorial factor of $\binom{n}{r-1}$ for the number of $(n-r+1)$ -bubble subdiagrams, we find after subtracting all counterterm insertions that the n -bubble (i.e. $(n+1)$ -loop) contribution to this diagram is given by the expression:

$$B_n = \frac{\kappa^n}{\epsilon^{n+1}} G(\epsilon) \sum_{r=1}^{n+1} r^{-1} (1 - r\epsilon) \Gamma(1 + r\epsilon) \Gamma(1 - r\epsilon) \binom{n}{r-1} (-1)^{r+1} x^{r\epsilon}. \quad (\text{A.4})$$

(We have also incorporated into this expression a factor of $(-1)^{L+1}$ for an L -loop diagram, which derives from the D -algebra.)

We now write[11]

$$(1 - r\epsilon)\Gamma(1 + r\epsilon)\Gamma(1 - r\epsilon)x^{r\epsilon} = \sum_{j=0}^{\infty} L_j(r\epsilon)^j. \quad (\text{A.5})$$

Substituting in Eq. (A.4), and using the identity

$$\begin{aligned} \Delta_j &= \sum_{r=1}^{n+1} r^{j-1} \binom{n}{r-1} (-1)^r = 0 \quad \text{when } j = 1, 2, \dots, n \\ &= -(n+1)^{-1} \quad \text{when } j = 0 \end{aligned} \quad (\text{A.6})$$

(which is proved in Appendix B) we find that the pole terms in B_n are given by the expression

$$B_n^{\text{pole}} = \frac{\kappa^n}{(n+1)\epsilon^{n+1}} \sum_{i=0}^n G_i \epsilon^i \quad (\text{A.7})$$

where we have written $G(\epsilon) = \sum G_n \epsilon^n$. The identity Eq. (A.6) removes all the non-local (i.e. $\ln x$ -dependent) counter-terms. Now we want to sum over n . In a β -function or anomalous dimension calculation, the result will be given by the coefficient of the simple pole in ϵ in the quantity $\sum (n+1) B_n^{\text{pole}}$, which is easily seen to give

$$B(\kappa) = \sum_{n=0}^{\infty} G_n \kappa^n = G(\kappa). \quad (\text{A.8})$$

Next we consider Fig. 3(A). A complication as compared with the calculation for Fig. 3(B) is that there are now two types of divergent subdiagram; in addition to those consisting of subsets of bubbles, there is also a divergent $(n+1)$ -loop subdiagram formed by erasing the upper propagator in Fig. 3(A). In fact this subdiagram is precisely the diagram Fig. 3(B), and therefore produces a counterterm B_n^{pole} as in Eq. (A.7). We therefore find that the n -bubble (or $(n+2)$ -loop) contribution to the diagram is given by

$$\begin{aligned} A_n &= \frac{\kappa^n}{\epsilon^{n+2}} \sum_{r=2}^{n+2} (-1)^{r-1} \binom{n}{r-2} \frac{H(\epsilon)^2}{1-\epsilon} \frac{1}{r(r-1)} \frac{\Gamma(1-\epsilon+r\epsilon)\Gamma(1+\epsilon-r\epsilon)\Gamma(1+r\epsilon)}{\Gamma(1-2\epsilon+r\epsilon)} x^{r\epsilon} \\ &\quad + \frac{\kappa^n}{\epsilon^{n+2}} \frac{1}{n+1} \sum_{i=0}^n (G_i \epsilon^i) \frac{\Gamma(2-2\epsilon)}{\Gamma(1-\epsilon)^2} x^\epsilon, \end{aligned} \quad (\text{A.9})$$

where

$$H(\epsilon) = \Gamma(2 - \epsilon)G(\epsilon), \quad (\text{A.10})$$

with $G(\epsilon)$ as in Eq. (A.3). As for Fig. 3(B), we have also incorporated a factor $(-1)^{L+1} = (-1)^{n+3}$ generated by the D -algebra. We may now extend the summation in the second term to infinity, at the expense of introducing one extra simple pole term together with finite terms. We obtain, up to finite terms,

$$\begin{aligned} A_n &= \frac{\kappa^n}{\epsilon^{n+2}} \sum_{r=2}^{n+2} (-1)^{r-1} \binom{n}{r-2} \frac{H(\epsilon)^2}{1-\epsilon} \frac{1}{r(r-1)} \frac{\Gamma(1-\epsilon+r\epsilon)\Gamma(1+\epsilon-r\epsilon)\Gamma(1+r\epsilon)}{\Gamma(1-2\epsilon+r\epsilon)} x^{r\epsilon} \\ &\quad + \frac{\kappa^n}{\epsilon^{n+2}} \frac{1}{n+1} \frac{H(\epsilon)^2}{1-\epsilon} \frac{\Gamma(1+\epsilon)}{\Gamma(1-\epsilon)} x^\epsilon - \frac{\kappa^n}{\epsilon} \frac{1}{n+1} G_{n+1} \\ &= \frac{1}{n+1} \frac{\kappa^n}{\epsilon^{n+2}} \sum_{r=2}^{n+2} (-1)^{r-1} r^{-1} \binom{n+1}{r-1} \frac{H(\epsilon)^2}{1-\epsilon} \frac{\Gamma(1-\epsilon+r\epsilon)\Gamma(1+\epsilon-r\epsilon)\Gamma(1+r\epsilon)}{\Gamma(1-2\epsilon+r\epsilon)} x^{r\epsilon} \\ &\quad + \frac{\kappa^n}{\epsilon^{n+2}} \frac{1}{n+1} \frac{H(\epsilon)^2}{1-\epsilon} \frac{\Gamma(1+\epsilon)}{\Gamma(1-\epsilon)} x^\epsilon - \frac{\kappa^n}{\epsilon} \frac{1}{n+1} G_{n+1}. \end{aligned} \quad (\text{A.11})$$

Rather remarkably, we now notice that the second term simply supplies the $r = 1$ term in the summation of the first term. We therefore obtain

$$\begin{aligned} A_n &= \frac{1}{n+1} \frac{\kappa^n}{\epsilon^{n+2}} \sum_{r=1}^{n+2} (-1)^{r-1} r^{-1} \binom{n+1}{r-1} \frac{H(\epsilon)^2}{1-\epsilon} \frac{\Gamma(1-\epsilon+r\epsilon)\Gamma(1+\epsilon-r\epsilon)\Gamma(1+r\epsilon)}{\Gamma(1-2\epsilon+r\epsilon)} x^{r\epsilon} \\ &\quad - \frac{\kappa^n}{\epsilon} \frac{1}{n+1} G_{n+1} + \text{finite terms}. \end{aligned} \quad (\text{A.12})$$

In the same spirit as for Fig. 3(B), we write

$$\frac{\Gamma(1-\epsilon+r\epsilon)\Gamma(1+\epsilon-r\epsilon)\Gamma(1+r\epsilon)}{\Gamma(1-2\epsilon+r\epsilon)} x^{r\epsilon} = \sum_{j=0}^{\infty} M_j(r\epsilon)^j. \quad (\text{A.13})$$

Substituting in Eq. (A.12), and using Eq. (A.6), we find

$$A_n = \frac{\kappa^n}{\epsilon^{n+2}} \frac{H(\epsilon)^2}{1-\epsilon} \frac{1}{(n+1)(n+2)} M_0 - \frac{\kappa^n}{\epsilon} \frac{1}{n+1} G_{n+1} + \text{finite terms}. \quad (\text{A.14})$$

Clearly from Eq. (A.13) we have $M_0 = \frac{\Gamma(1-\epsilon)\Gamma(1+\epsilon)}{\Gamma(1-2\epsilon)}$, and so, from Eqs. (A.3), (A.10), we find

$$\begin{aligned} A_n &= \frac{\kappa^n}{\epsilon^{n+2}} (1-2\epsilon) \frac{1}{(n+1)(n+2)} G(\epsilon) \\ &\quad - \frac{\kappa^n}{\epsilon} \frac{1}{n+1} G_{n+1} + \text{finite terms}. \end{aligned} \quad (\text{A.15})$$

As in the case of Fig. 3(B), the contribution to a β -function or anomalous dimension will be given by the coefficient of the simple pole in ϵ in the quantity $\sum (n+2)A_n$, giving

$$\begin{aligned} A(\kappa) &= \sum_{n=0}^{\infty} \frac{1}{n+1} (G_{n+1} - 2G_n) \kappa^n - \sum_{n=0}^{\infty} \frac{n+2}{n+1} G_{n+1} \kappa^n \\ &= - \sum_{n=0}^{\infty} \left[G_{n+1} + \frac{2}{n+1} G_n \right] \kappa^n, \end{aligned} \quad (\text{A.16})$$

which may be rewritten in the compact form

$$A(\kappa) = -\frac{1}{\kappa} \left[G(\kappa) - 1 + 2 \int_0^{\kappa} G(x) dx \right]. \quad (\text{A.17})$$

The calculation of $C(\kappa)$ parallels very closely that of $A(\kappa)$, and yields

$$C(\kappa) = -2\kappa^{-1} \left[G(\kappa) - 1 + \int_0^{\kappa} (1+2x)G(x) dx \right], \quad (\text{A.18})$$

The computation of Fig. 3(D) is somewhat different, however, and we shall explain it in detail. The n -bubble diagram together with its counterterms (in this case simply bubble-chains, as for Fig. 3(B)) gives

$$D_n = -(n+1) \frac{\kappa^n}{\epsilon^{n+1}} \sum_{r=3}^{n+3} \frac{(-1)^{r-1}}{r} \binom{n}{r-3} G(\epsilon) \Gamma(1-r\epsilon) \Gamma(1+r\epsilon) x^{r\epsilon}. \quad (\text{A.19})$$

The factor of $(n+1)$ represents the $(n+1)$ ways of distributing n bubbles in Fig. 3(D). Now we write

$$\Gamma(1-r\epsilon) \Gamma(1+r\epsilon) x^{r\epsilon} = \sum_{j=0}^{\infty} P_j(r\epsilon)^j. \quad (\text{A.20})$$

It is easy to see from Eq. (A.6) that

$$\sum_{r=3}^{n+3} (-1)^r r^{j-1} \binom{n}{r-3} = 0 \quad (\text{A.21})$$

for $j \geq 1$. This ensures the cancellation of non-local terms and leaves only the $j=0$ term. Using the result

$$\sum_{r=3}^{n+3} \frac{(-1)^r}{r} \binom{n}{r-3} = -\frac{2}{(n+1)(n+2)(n+3)}, \quad (\text{A.22})$$

which is proved in Appendix B, together with $P_0 = 1$, we have

$$D_n = -\frac{\kappa^n}{\epsilon^{n+1}} G(\epsilon) \frac{2}{(n+2)(n+3)}. \quad (\text{A.23})$$

The contribution to a β -function or anomalous dimension is then given by the simple pole in $\sum (n+3)D_n$, yielding

$$D(\kappa) = -2 \sum_{n=0}^{\infty} \frac{G_n}{n+2} \kappa^n, \quad (\text{A.24})$$

which may be rewritten

$$D(\kappa) = -\frac{2}{\kappa^2} \int_0^\kappa x G(x) dx. \quad (\text{A.25})$$

Appendix B. Summation identities

In this appendix we prove the identities Eqs. (A.6) and (A.22), which play a crucial rôle in disposing of non-local contributions and deriving the final bubble-sum results. Eq. (A.6) may be proved starting from

$$(1-x)^n = \sum_{r=0}^n (-1)^r x^r \binom{n}{r}. \quad (\text{B.1})$$

Differentiating Eq. (B.1) l times (where $l \leq n-1$), and setting $x = 1$, we obtain

$$0 = \sum_{r=0}^n (-1)^r r(r-1) \dots (r-l+1) \binom{n}{r}. \quad (\text{B.2})$$

Clearly, by taking linear combinations of Eq. (B.2) with different values of l , we may obtain

$$0 = \sum_{r=0}^n (-1)^r r^{j-1} \binom{n}{r} \quad (\text{B.3})$$

for $1 \leq j \leq n$. On the other hand, by integrating Eq. (B.1) we obtain

$$\frac{1}{n+1} = \sum_{r=0}^n (-1)^r (r+1)^{-1} \binom{n}{r}. \quad (\text{B.4})$$

Upon changing the summation range, Eqs. (B.3) and (B.4) are clearly equivalent to Eq. (A.6), namely

$$\begin{aligned} \Delta_j &= \sum_{r=1}^{n+1} r^{j-1} \binom{n}{r-1} (-1)^r = 0 \quad \text{when } j = 1, 2, \dots, n \\ &= -(n+1)^{-1} \quad \text{when } j = 0. \end{aligned} \quad (\text{B.5})$$

Upon integrating the identity

$$x^2(1-x)^n = \sum_{r=0}^n (-1)^r \binom{n}{r} x^{r+2}, \quad (\text{B.6})$$

and then setting $x = 1$, we obtain

$$\sum_{r=0}^n \frac{(-1)^r}{r+3} \binom{n}{r} = \frac{2}{(n+1)(n+2)(n+3)}, \quad (\text{B.7})$$

which is equivalent to Eq. (A.22).

Acknowledgements

PF was supported by a scholarship from JNICT, and CGN by a PPARC studentship. We thank John Gracey for several useful discussions.

References

- [1] E. Witten, Ann. Phys. 128 (1980) 363
- [2] J. Zinn–Justin, Phys. Reports 70 (1981) 110
- [3] J.J.M. Verbaarschot and P. West, Phys. Rev. **D42** (1990) 1276; *ibid* **D43** (1991) 2718
- [4] J.J.M. Verbaarschot and P. West, Int. J. Mod. Phys. **A6** (1991) 2361
- [5] A.N Vasil’ev, Yu.M. Pis’mak and J.R. Honkonen, Theor. Math. Phys. 46 (1981) 157; *ibid* 47 (1981) 291
- [6] J.A. Gracey, Nucl. Phys. **B352** (1991) 183
- [7] J.A. Gracey, Int. J. Mod. Phys. **A8** (1993) 2465; Phys. Lett. **B373** (1996) 173; Nucl. Phys. **B414** (1994) 614
- [8] C. Bagnuls and C. Bervillier, hep-th/9702149
- [9] P.M. Ferreira, I. Jack, and D.R.T. Jones, hep-ph/9702304
- [10] W. Siegel, Phys. Lett. **B84** (1979) 193;
D.M. Capper, D.R.T. Jones and P. van Nieuwenhuizen, Nucl. Phys. **B167** (1980) 479
- [11] A. Palanques-Mestre and P. Pascual, Comm. Math. Phys. 95 (1984) 277
- [12] I. Jack, D.R.T. Jones and C.G. North, Nucl. Phys. **B486** (1997) 479
- [13] I. Jack, D.R.T. Jones and C.G. North, Nucl. Phys. **B473** (1996) 308
- [14] P.M. Ferreira, I. Jack, and D.R.T. Jones, Phys. Lett. **B392** (1997) 376
- [15] P.S. Howe, K.S. Stelle and P. West, Phys. Lett. **B124** (1983) 55;
P.S. Howe, K.S. Stelle and P.K. Townsend, Nucl. Phys. **B236** (1984) 125
- [16] D.R.T. Jones, Nucl. Phys. **B87** (1975) 127
- [17] A. Belavin and A. Migdal, JETP Lett. 19 (1974) 181;
W. Caswell, Phys. Rev. Lett. 33 (1974) 244;
D.R.T. Jones, Proceedings, Recent Progress In Lagrangian Field Theory and Applications, Marseille 1974, 68
- [18] N. Seiberg, Nucl. Phys. **B435** (1995) 129
- [19] I. Jack, D.R.T. Jones and M.A. Samuel, in preparation
- [20] J. Ellis, M. Karliner and M.A. Samuel, hep-ph/9612202
- [21] W. Siegel, Phys. Lett. **B94** (1980) 37;
L.V. Avdeev, G.A. Chochia and A.A. Vladimirov, Phys. Lett. **B105** (1981) 272.